Quantum scattering theory on the momentum lattice

O. A. Rubtsova,* V. N. Pomerantsev,† and V. I. Kukulin‡
Institute of Nuclear Physics, Moscow State University, Leninskie Gory, RU-119991 Moscow, Russia
(Received 11 December 2008; revised manuscript received 18 February 2009; published 10 June 2009)

A new approach based on the wave-packet continuum discretization method recently developed by the present authors for solving quantum-mechanical scattering problems for atomic and nuclear scattering processes and few-body physics is described. The formalism uses the complete continuum discretization scheme in terms of the momentum stationary wave-packet basis, which leads to formulation of the scattering problem on a lattice in the momentum space. The solution of the few-body scattering problem can be found in the approach from linear matrix equations with nonsingular matrix elements, averaged on energy over lattice cells. The developed approach is illustrated by the solution of numerous two- and three-body scattering problems with local and nonlocal potentials below and well above the three-body breakup threshold.

DOI: 10.1103/PhysRevC.79.064602 PACS number(s): 03.65.Nk, 21.45.−v, 24.10.Ht

I. INTRODUCTION

For the last couple of decades, many different methods have been formulated to solve the quantum mechanical scattering problems with a few particles in continuum for precise quantitative treatment of numerous atomic, nuclear, and hadronic processes. Such "exact" formulations in the field of atomic and nuclear processes have been addressed mainly to go beyond the well-known distorted-wave Born approximation (DWBA) approach or to justify the specific employment of the respective approximation schemes (e.g., the coupled-channel approaches.). In principle, the rigorous Faddeev and Merkuriev-Faddeev equations for three-body scattering and the generalized Faddeev-Yakubovsky four- and few-body equations do solve the basic scattering problem. However, their practical implementation on realistic cases (in atomic and nuclear physics) often meets with such serious difficulties caused by the presence of complicated optical-model input potentials, long-range Coulomb interactions, effective many-body forces, etc., that to date only a rather limited class of practical cases has been treated on the basis of exact few-body scattering equations.[1] These difficulties relate mainly to the account of three- or four-body breakup channels in elastic and inelastic electron-atom, electron-molecule, or hadron-nucleus and nucleus-nucleus collisions, especially in the case of charged particles, where long-range Coulomb interactions make the quantitative treatment even more involved.

Thus, the development of alternative practically effective approaches toward solving the few-body scattering problems in atomic and nuclear reaction studies is still of great importance. Our interest here is on methods that make use of a basis of square-integrable functions (i.e., of the L_2 space),[2] which historically have been developed for atomic physics purposes [5–10] and adapted to nuclear physics processes [11,12]. Such methods allow one to represent operators and wave functions by matrices and vectors on the chosen basis subspace and formulate the scattering problems in terms of matrix equations rather than solving the initial exact integral or differential ones in the momentum or coordinate spaces. In general, the employment of only L_2-type basis in the scattering problem makes the solution of few-body scattering problems to be quite similar to the treatment of bound-state problems. As for the latter, the modern few- and many-body techniques make it possible to treat very precisely bound-state problems with many tens or even hundreds of particles. So we believe that the development of L_2-type techniques is a very promising way for treating scattering problems with few particles in continuum most effectively and with the use of modern personal computers instead of powerful supercomputers.

Furthermore, as was mentioned by Wigner [13] and Messiah [14], an incorporation of continuous spectrum (scattering) states into rigorous quantum mechanical formulation is possible in terms of L_2 (or normalizable) wave functions only. Indeed, the conventional scattering states do not belong to the Hilbert space, and the basic properties of Hamiltonian (even Hermitian property) could not be established using such non-normalizable states [14]. Thus, to operate with nonvanishing at infinity and non-normalizable continuum wave functions, one should proceed in the following way, according to the Wigner idea [13]. One has to divide the whole continuous spectrum of the Hamiltonian into nonoverlapping energy intervals of small width Δ (i.e., *discretize* the continuum) and construct the so-called eigendifferentials, i.e., integrals of the continuum wave functions over each interval. Then, all the continuum wave function properties can be proved for the set of eigendifferentials; and after passing to the $\Delta \to 0$ limit, one

*rubtsova@nucl-th.sinp.msu.ru
†pomeran@nucl-th.sinp.msu.ru
‡kukulin@nucl-th.sinp.msu.ru

[1] Although the treatment of fully realistic NN and $3N$ interactions for $3N$- and $4N$-scattering cases has been realized for last two decades [1–4].

[2] We do not refer here to the applications of the very numerous variational methods to scattering problems, but rather to the so-called direct methods only, where the scattering wave functions (including their asymptotic parts) are expanded directly into L_2-basis functions.

can extend these properties to the non-normalizable scattering states [13].

Keeping in mind this Wigner's discretization procedure, we developed a new approach to general quantum scattering theory [15–20] that uses directly the above eigendifferential states as the L_2 basis in which framework the few-body scattering problems can be formulated in the Hilbert space. We renamed them *stationary wave packets* because the name looks now more physical and clear for understanding. The approach developed—the wave-packet continuum discretization method (WPCD)—combines both the advantages of the above L_2 techniques and accurate direct solution methods of the rigorous few-body equations. Indeed, on the one hand, the WPCD method uses matrix representations for the scattering theory operators and allows us to reduce the solution of the initial scattering problem to solving matrix equations in L_2 wave-packet subspace. On the other hand, these matrix equations[3] correspond to some regularization of the exact integral scattering equations, because integral kernel singularities are averaged and smoothed over energy (or momentum) bins. So, from this point of view, the WPCD method can be considered as an effective quadrature technique for the solution of integral scattering equations in the momentum space.

This "duality" also allows us to obtain diagonal matrix approximations for two- and few-body channel resolvents, which behave properly as functions of energy, using the direct explicit relationship between the above L_2 wave-packet functions and corresponding exact scattering wave functions. By further replacing these energy-dependent discretized resolvents by a respective matrix with elements averaged over each energy bin, one gets fully energy-discretized (i.e., histogram-like) representations for other scattering operators and wave functions in the momentum space as well [15–20]. This makes it possible to formulate the novel completely discrete formalism for a treatment of the quantum scattering *on the momentum lattice*. In this formalism, all the scattering operators take the form of finite matrices, while their energy and momentum dependences are averaged over lattice cells.[4]

It is argued that such a purely discrete lattice representation of the scattering amplitude can describe real scattering experiments more adequately than the traditional continuous representation because of finite energy and angular resolutions of all instruments used in measurements for such experiments. So, the main idea behind the present wave-packet technique is to operate with some *properly averaged quantities* (wave functions, operators, etc.) instead of handling exact quantities linked to the continuous spectrum, which have complicated energy singularities in the few-body case.

As has been previously demonstrated [18–20], the general wave-packet technique can be straightforwardly applied to three- and many-body scattering problems by constructing respective three- and many-body wave-packet bases. So, this technique makes it possible to greatly facilitate the solution of the respective few-body scattering problems. Moreover, the approach leads to quite universal finite-dimensional formulation of any scattering problem on the purely L_2-type basis. We recently demonstrated the high efficiency of this discretization technique applied to the scattering of a composite particle off a nuclear target [15,20], showing that it is a good alternative to the traditional coupled-channel approach. However, in that work, we addressed mainly the detailed comparison with the results of conventional approaches [mainly the continuum-discretized coupled-channel (CDCC) method [21–24]] used in the field, and thus we omitted there almost all the details of the wave-packet technique. So, in the present paper, we detail the whole approach and introduce a more general basis for continuum discretization—a discrete momentum-bin basis for few-body scattering calculations. Eventually we demonstrate here the effectiveness of the technique by considering a few tests in the field of two- and three-body scattering above the breakup threshold.

The present paper is organized as follows. In Sec. II, we introduce the generalized stationary wave-packet basis, study its properties, and define the details of the discretization procedure. In Sec. III, the discrete analogs of the basic scattering operators and the finite-dimensional approximation for the scattering amplitude are derived. The validity of the method for a nonlocal two-body interaction is tested in Sec. IV. In Sec. V, the three-body elastic scattering problem with separable pairwise interactions both below and above the breakup threshold is studied and compared with published results. In Sec. VI, we extend our method to solving the general three-body problem and introduce the three-body lattice basis. The summary of the results attained is presented in Sec. VII.

II. GENERALIZED STATIONARY WAVE PACKETS AND THEIR BASIC PROPERTIES

First of all, we construct the basis for discretization of a two-body continuous spectrum. The two-body system Hamiltonian is assumed to be in conventional form

$$h = h_0 + v, \tag{1}$$

where h_0 is the free Hamiltonian and v is the short-range interaction potential. We assume that the potential v is spherically symmetrical. Further we will consider the h_0 eigenstates $|\psi_{0q}^{LM}\rangle \equiv |\psi_{0q}^{L}, Y_{LM}\rangle$ corresponding to the given values L of the angular momentum $\mathbf{L}$ and its projection M onto the z axis (here Y_{LM} are the usual spherical functions given in the coordinate or momentum representation). Because values L and M are conserved, we will mainly discuss the radial parts of the wave functions $|\psi_{0q}^{L}\rangle$ in what follows.

[3]It should be stressed that the matrix equations describing the scattering processes in our approach are of different type than the matrix equations derived from the conventional quadrature discretization of, e.g., the Lippmann-Schwinger integral equation, because in our case the matrices represent the scattering operators themselves.

[4]Contrary to this discretization procedure, which is specific to the lattice representation, in conventional discretization methods one simply takes the momentum variables (in the integral equation kernel) to be in some fixed grid points.

A. Stationary wave packets (eigendifferentials)

Let us confine the continuous spectrum of h_0 (at each partial wave L) within the maximal value $E_{\max}$ and divide the interval $[0, E_{\max}]$ into a finite number of nonoverlapping energy bins $[\mathcal{E}_{i-1}, \mathcal{E}_i]_{i=1}^N$ (with $\mathcal{E}_0 = 0$ and $\mathcal{E}_N = E_{\max}$). Here we assume that the value $E_{\max}$ is sufficiently large to provide a proper solution of the discussed problem (for details, see the next subsection). Each such energy bin corresponds to the momentum (or wave number) interval $[q_{i-1}, q_i]$ on momentum axis q, where $q = \sqrt{2\mu E}$ and μ is the reduced mass. Consider further a complete set of the h_0 continuum states $|\psi_{0q}^L\rangle$ (plane waves), which are normalized according to the Dirac δ function on the momentum value q:

$$\langle \psi_{0q}^{LM} | \psi_{0q'}^{L'M'} \rangle = \delta(q - q')\delta_{LL'}\delta_{MM'}. \tag{2}$$

Now let us define a set of *free* stationary wave packets (WPs) as integrals of the plane waves (corresponding to the *free* motion) over the above momentum bins:

$$|x_i^L\rangle = \frac{1}{\sqrt{B_i}} \int_{q_{i-1}}^{q_i} dq f(q) |\psi_{0q}^L\rangle, \quad i = 1, \ldots, N, \tag{3}$$

where $f(q)$ is some weight function and B_i are normalization factors, directly interrelated to each other:

$$B_i = \int_{q_{i-1}}^{q_i} dq\, |f(q)|^2. \tag{4}$$

The main advantage of the "packetizing procedure" defined in Eq. (3) is that wave-packet functions belong to L_2 space, i.e., they are normalizable in a usual sense (similar to the bound-state functions) and are vanishing at infinity in contrast to the initial plane waves. Thus, wave-packet functions belong to a Hilbert space. Different choices of weight function lead to different sets of WPs. In our previous papers [16–20], the basis of the energy packets $|X_i\rangle$ was used for which the weight functions and normalization factors are defined as

$$f(q) = \sqrt{\frac{q}{\mu}}, \quad B_i = \frac{q_i^*}{\mu} d_i \equiv D_i, \tag{5}$$

where $D_i \equiv \mathcal{E}_i - \mathcal{E}_{i-1}$ are the energy interval widths, $d_i \equiv q_i - q_{i-1}$ are the momentum bin widths, and $q_i^* = \frac{1}{2}(q_{i-1} + q_i)$ are the bin midpoints. Explicit formulas for the scattering operators on the energy-packet representation can be found in Refs. [16–20].

So, the main focus in the present paper is the momentum packet representation which is more convenient for the few-body continuum discretization, where the *momentum* packets (q packets) $|x_i^L\rangle$ with unit weight functions are used. In this case, the normalization factor B_i in Eq. (3) is just equal to the bin width d_i:

$$B_i = d_i, \quad f(q) = 1. \tag{6}$$

Let us consider further the basic properties of the WP $|x_i^L\rangle$. The overlapping between WP functions can be calculated using the definition (3) and the orthogonality property (2) of the initial plane waves:

$$\langle x_i^L | x_j^L \rangle = \frac{1}{\sqrt{B_i B_j}} \int_{q_{i-1}}^{q_i} \int_{q_{j-1}}^{q_j} dq\, dq'\, f^\dagger(q) f(q') \delta(q - q').$$

The δ function under the integral is not vanishing only if both intervals i and j coincide (they are nonoverlapping), i.e., when $i = j$. So, one finds the relation

$$\langle x_i^L | x_j^L \rangle = \delta_{ij} \frac{1}{B_i} \int_{q_{i-1}}^{q_i} dq |f(q)|^2.$$

Using the definition (4), we conclude that the set $|x_i^L\rangle_{i=1}^N$ is orthonormalized:

$$\langle x_i^L | x_j^L \rangle = \delta_{ij}, \quad i, j = 1, \ldots, N. \tag{7}$$

We will call the linear subspace spanned by the set of WP $\{|x_i^L\rangle_{i=1}^N\}$ as the wave-packet subspace (WPS). The projector onto the WPS has the evident form

$$\mathfrak{p}_L = \sum_{i=1}^N |x_i^L\rangle\langle x_i^L|. \tag{8}$$

Further we will use the projections of scattering operators onto the WPS and denote them by corresponding gothic letters similar to the projector $\mathfrak{p}_L$.

Using definition (3), one gets the projective rule for the wave-packet basis

$$\mathfrak{p}_L |\psi_{0q}^L\rangle = \begin{cases} \dfrac{f(q)}{\sqrt{B_k}} |x_k^L\rangle, & q \in [q_{k-1}, q_k], \\ 0, & q > q_N. \end{cases} \tag{9}$$

Thus the projection of a plane wave is proportional to the single WP function, corresponding to that interval to which the on-shell momentum value q belongs. Below we will denote this interval with the index k.

The property in Eq. (9) allows us to find in closed form the eigenvalues for the projection of any operator R, which has an explicit functional dependence of h_0. Indeed, the spectral expansion for such an operator takes the form

$$R(h_0) = \sum_{L=0}^\infty \int_0^\infty dq |\psi_{0q}^L\rangle R\left(\frac{q^2}{2\mu}\right) \langle \psi_{0q}^L|.$$

Now let us apply the above projection operators $\mathfrak{p}_L$ onto the WPS from the right and from the left. As a result, one obtains the following *diagonal form* for the projection of the operator R for the fixed partial wave L [using Eq. (9)]:

$$\mathfrak{R} \equiv \mathfrak{p}_L R(h_0) \mathfrak{p}_L = \sum_{i=1}^N |x_i^L\rangle R_i \langle x_i^L|, \tag{10}$$

where the corresponding eigenvalues R_i are defined as

$$R_i \equiv \langle x_i^L | R(h_0) | x_i^L \rangle = \frac{1}{B_i} \int_{q_{i-1}}^{q_i} dq\, R\left(\frac{q^2}{2\mu}\right) |f(q)|^2. \tag{11}$$

In particular, the free Hamiltonian eigenvalues in WP basis are equal to

$$\langle x_i^L | h_0 | x_i^L \rangle \equiv \epsilon_i^* = \frac{1}{B_i} \int_{q_{i-1}}^{q_i} dq\, |f(q)|^2 \frac{q^2}{2\mu}. \tag{12}$$

For the q packets, these eigenvalues are defined by the simple formula

$$\epsilon_i^* = \frac{(q_i^*)^2}{2\mu} \left(1 + \frac{(d_i)^2}{12(q_i^*)^2}\right). \tag{12a}$$

The most useful property of the WP basis for solving the scattering equations is the finite-dimensional representation for the resolvent of the free Hamiltonian $g_0(E) = [E + i0 - h_0]^{-1}$, that is,

$$\mathfrak{g}_0(E) \equiv \mathfrak{p}_L g_0(E) \mathfrak{p}_L = \sum_{i=1}^{N} |x_i^L\rangle g_i(E) \langle x_i^L|. \tag{13}$$

Here the corresponding complex-valued eigenvalues $g_i(E)$ have the definition

$$g_i(E) = \frac{1}{B_i} \int_{q_{i-1}}^{q_i} dq' \frac{|f(q')|^2}{E + \mathrm{i}0 - \frac{q'^2}{2\mu}}. \tag{14}$$

For q packets, these integrals can be easily calculated analytically:

$$g_i(E) = \frac{\mu}{q d_i} \left\{ \ln \left| \frac{q - q_{i-1}}{q - q_i} \right| + \ln \left| \frac{q + q_i}{q + q_{i-1}} \right| - i\pi \left[\theta(q - q_{i-1}) - \theta(q - q_i) \right] \right\}, \tag{15}$$

where $q = \sqrt{2\mu E}$ and the combination of the Heaviside θ functions[5] means that the imaginary part of the eigenvalues does not vanish only in a single interval with $i = k$ to which the respective on-shell momentum value q belongs, i.e., $q \in [q_{k-1}, q_k]$. Because the integrand in Eq. (14) has a singularity at $q' = q$, we refer to this interval as a *singular* one. Although the eigenvalue (15) has logarithmic singularities if q is equal to one of the singular bin endpoints, the finite-dimensional (f.-d.) representation (13) for the free resolvent with eigenvalues (15) can be used directly to obtain scattering observables. We assume here that energy E does not coincide with any energy-bin endpoint [16]. Further (in Sec. II C) we will introduce some averaging (on energy) procedure and derive the averaged f.-d. representation for the free resolvent which has no singularities at all on the real energy axis.

Using this finite-dimensional packet analog (13) for the free resolvent, one can build easily the f.-d. scheme for solution of the general scattering problem. Below we will restrict our formulation basically to the q-packet basis, because the formalism based on the energy packet basis has been discussed in our previous papers [15,16,18–20].

We should mention that WP states can be constructed not only for the free Hamiltonian h_0 but also for any Hamiltonian h_1 using the same discretization procedure, that is,

$$|z_i^L\rangle = \frac{1}{\sqrt{A_i}} \int_{q_{i-1}}^{q_i} dq\, w(q) |\psi_q^L\rangle, \quad i = 1, \ldots, N, \tag{3a}$$

where the $|\psi_q^L\rangle$ are eigenstates of the continuous spectrum of h_1. To distinguish these *scattering* wave packets from the free ones, we denote them by another letter. The properties of the scattering WPs are absolutely the same as those of the free WPs. Jointly with bound states of h_1 (if they exist), the set of $\{|z_i^L\rangle\}_{i=1}^N$ states form a basis in a Hilbert space in which any operator commuting with Hamiltonian h_1 has a diagonal f.-d. representation [16].

B. Behavior of the q packets in the coordinate and momentum spaces

It is easy to show that the q-packet basis functions $|x_i^L\rangle$ are vanishing at large distances in the coordinate space in contrast to the exact plane waves $|\psi_{0q}^L\rangle$ and they approximately coincide with the latter in some inner area.

The radial part of a free wave function in the coordinate representation has the form

$$\psi_{0q}^L(r) = \sqrt{\frac{2}{\pi}} q\, j_L(qr), \tag{16}$$

where j_L is a spherical Bessel function. For simplicity, we consider at first the s-wave case, when an explicit relation between the initial plane wave and the wave-packet functions can be derived. Let us put the form (16) into the definition of free wave packets in Eq. (3):

$$x_i^0(r) = \frac{1}{\sqrt{d_i}} \int_{q_{i-1}}^{q_i} \sqrt{\frac{2}{\pi}} \frac{\sin(qr)}{r} dq, \quad qr \gg 1.$$

One gets immediately from this definition an exact relation for the exact q packets and initial plane waves, i.e.,

$$x_i^0(r) = \sqrt{d_i} \psi_{0q_i^*}^0(r) \frac{\sin(d_i r/2)}{d_i r/2}, \tag{17}$$

where q_i^* is the bin midpoint. It is clear from Eq. (17) that the q packets $x_i^0(r)$ nearly coincide with the exact free solutions $\psi_{0q_i^*}^0(r)$ in the region $r \ll r_i$, where

$$r_i = \frac{2}{d_i}. \tag{18}$$

Thus, the "packetizing" procedure in Eq. (3) of initial plane waves leads to the additional decreasing factor in the WP function, which provides normability of the WP states.

For nonzero angular momentum L, the relation similar to Eq. (17) can be derived using the asymptotic form of the free-motion wave functions of Eq. (16), i.e.,

$$x_i^L(r) = \frac{1}{\sqrt{d_i}} \int_{q_{i-1}}^{q_i} \sqrt{\frac{2}{\pi}} \frac{\sin\left(qr - \frac{L\pi}{2}\right)}{r} dq, \quad qr \gg 1.$$

So by repeating the above derivation for the s-wave case, one finds that the WP function nearly coincides with the exact free-motion wave function in the bin midpoint momentum q_i^* over the region $\frac{1}{q_i^*} \ll r \ll r_i$.[6]

Thus, one can use the above q-packet states $|x_i^L\rangle$ instead of the exact plane waves ψ_{0q}^L in integral kernels of scattering operators if the range of the interaction v is less than $r_{\min} = \min_i r_i$.

[5] We use here the Heaviside θ function which is defined as $\theta(q) = \begin{cases} 1, & q \geqslant 0 \\ 0, & q < 0 \end{cases}$.

[6] Let us mention that this double inequality makes sense for most bins, because in practice we use meshes with $d_i \ll q_i^*$. Only on the first bin, where $d_0 = 2q_0^*$, the WP function differs strongly from the initial plane wave. But this fact does not corrupt the whole scheme.

Now the natural question arises: does the q-packet set $|x_i^L\rangle_{i=1}^N$ form a complete basis (for the fixed partial wave)? In the full coordinate space, of course not. It is clear, however, that when we replace the exact unit operator I_L, which can be written as

$$I_L \equiv \sum_{i=1}^{N} I_i + I_{\rm r} = \sum_{i=1}^{N} \int_{q_{i-1}}^{q_i} |\psi_{0q}^L\rangle\langle\psi_{0q}^L| dq + \int_{q_N}^{\infty} |\psi_{0q}^L\rangle\langle\psi_{0q}^L| dq, \quad (19)$$

by the wave-packet projection operator $\mathfrak{p}_L$, we are making herewith two approximations:

(i) The infinite continuous spectrum is truncated with the maximal value q_N, and the residual integral $I_{\rm r}$ is neglected.
(ii) The exact partial spectral projectors I_i are replaced by WP partial projectors $|x_i^L\rangle\langle x_i^L|$.

Surely, these two assumptions are not valid for the full Hilbert space. But keeping in mind practical applications of the method, one can compare the mean values of operators I and $\mathfrak{p}_L$ in some L_2 normalized state $|\Phi\rangle$ with an effective range r_0. To satisfy the conditions

$$\langle\Phi|\mathfrak{p}_L|\Phi\rangle \approx \langle\Phi| \sum_{i=1}^{N} I_i |\Phi\rangle, \quad \langle\Phi|I_t|\Phi\rangle \approx 0, \quad (20)$$

one has to choose sufficiently small widths d_i and sufficiently high maximal momentum q_N values:

$$d_i \ll \frac{1}{r_0} \ll q_N, \quad i = 1, \ldots, N. \quad (21)$$

With these restrictions, one can take for the practical realization the proper conditions for the momentum bin partition $[q_{i-1}, q_i]_{i=1}^N$. Then one can check the convergence of the results with increasing the wave-packet basis dimension, when the bin widths become smaller, and the maximum value q_N becomes higher.

As we approximate infinite spectral integrals by the discrete finite sums, the WP method seems very similar to the techniques for evaluating integrals (also with singularities) by constructing quadratures [25,26]. Quadrature methods also lead to discretization of integrals and use some effective momentum or energy meshes. In the quadrature language, WP mesh points are the bin midpoints and WP weights are just the bin widths. But the essential differences of the present WP technique from the previous quadrature methods is the incorporation of the specific L_2 WP basis and the representation of scattering operators themselves by matrices in that basis, instead of representing them by the values of the kernels at the momentum mesh points. In particular, this basis WP representation leads to a simple analytical diagonal form for the free (or channel, in the few-body case) resolvent matrix.

In Fig. 1, the coordinate behaviors of the free wave-packet functions for cases of broad, intermediate, and narrow bins are given (for $L = 0$). It is evident that these L_2-type functions are not vanishing at a very far asymptotic region up to

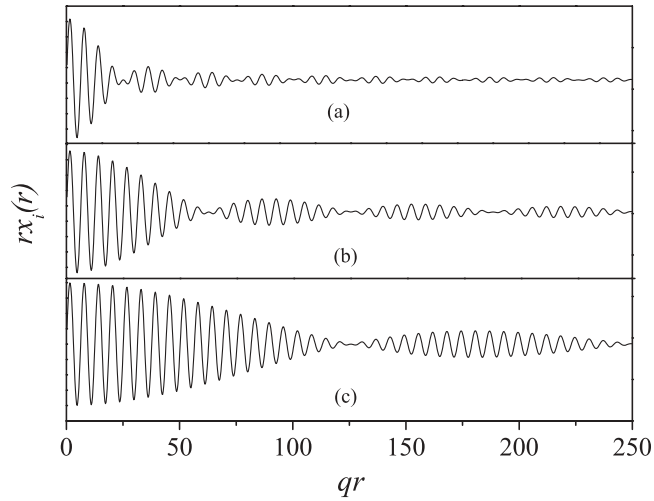

FIG. 1. Coordinate behavior of the dimensionless s-wave WP function $rx_i(r)$ for different values of the bin width d_i (in ratio to the momentum value q). (a) $d_i/q = 0.25$, (b) $d_i/q = 0.1$, and (c) $d_i/q = 0.05$.

$qr \sim 200$. Thus, the wave-packet basis is very suitable for the expansion of continuous spectrum wave functions. This long-range behavior of the basis functions plays a crucial role in the three-body scattering, especially above the breakup threshold, because it provides a proper overlapping between basis functions in different Jacobi-coordinate sets.

The most interesting picture arises in momentum space, where the q packets are represented just by the step-like functions

$$x_i^L(q) = \frac{\theta(q - q_{i-1}) - \theta(q - q_i)}{\sqrt{d_i}}, \quad i = 1, \ldots, N. \quad (22)$$

Such a particular discretization of the energy spectrum leads to a discrete momentum dependence for the scattering wave functions and the operator kernels. From this point of view the above wave-packet representation is *the discrete momentum representation*. On the other hand, if the momentum takes discrete values only, a direct analogy with the solid state physics arises. Indeed, the momentum space in the WP scheme becomes a lattice, which is one dimensional in the two-body and multidimensional in the few-body scattering. Further, the integral operators are represented in this scheme by their matrices, whose elements are integrals of the operator kernels over momentum lattice cells. By such an integration, the kernel singularities are averaged over momentum cells and smoothed.

Thus, one can treat the wave-packet formalism developed just as some finite-dimensional lattice representation for solving singular integral equations in quantum scattering problems.

Now we will turn to the concrete discretization procedure, which will be used in solving scattering equations.

C. Details of the discretization procedure

The discretization procedure suggested in the WPCD method [15–20] consists of the following steps:

(i) All scattering wave functions (for free and total Hamiltonians) are represented by their expansions in the wave-packet basis.
(ii) The respective operators are represented by their f.-d. projections onto the WPS.
(iii) The packetized objects are substituted into the scattering integral equations which become now the matrix ones.

From first glance, such an expansion of the nonnormalizable (in the L_2 space) scattering wave functions over the *finite set* of L_2 wave-packet functions seems nonconvergent in principle. But this expansion has meaning because only the inner parts of the scattering wave functions are required to find the scattering observables for a short-range potential v. Indeed, the scattering amplitude can be found from the well-known formula

$$A(E) \sim \langle \psi_{0q}^{L} | v | \psi_{q}^{L(+)} \rangle,$$

where $|\psi_q^{(+)}\rangle$ is the scattering wave function. It is clear that the external part of this function (as well as that of the free solution) is effectively cut off due to the vanishing potential v beyond some radius r_0. Thus, if the restrictions in Eq. (21) for the WP basis are satisfied for the potential effective range r_0, the above discretization procedure looks rather rational.

In the wave-packet scheme, the spectrum of the projected Hamiltonian is fully discrete and the momentum space is a lattice. So to make the scheme fully self-consistent, it is desirable to make the energy (which enters the resolvents as a parameter) also discrete. Thus we define *the averaged discretization procedure* in which the energy-dependent f.-d. approximation for the free resolvent [Eq. (13)] is averaged over energy inside the singular bin k ($E \in [\mathcal{E}_{k-1}, \mathcal{E}_k]$):

$$\mathfrak{g}_0^{(k)} = \frac{1}{D_k} \int_{\mathcal{E}_{k-1}}^{\mathcal{E}_k} \mathfrak{g}_0(E)\, dE = \sum_{i=1}^{N} |x_i^L\rangle g_i^{(k)} \langle x_i^L|, \tag{23}$$

where the energy-averaged eigenvalues are defined by the integral

$$g_i^{(k)} \equiv \frac{1}{D_k} \int_{q_{k-1}}^{q_k} g_i(q) \frac{q}{\mu}\, dq. \tag{24}$$

Explicit formulas for the q-packet case now are the following:

$$g_i^{(k)} = \frac{1}{D_k d_i} \left[Q_{ki}^{(+)} - Q_{ki}^{(-)} \right] - \frac{i\pi}{D_k} \delta_{ik}, \tag{25}$$

where

$$Q_{ki}^{(\pm)} = \sum_{k'=k-1}^{k} \sum_{i'=i-1}^{i} (-1)^{k-k'+i-i'} [q_{k'} \pm q_{i'}] \ln |q_{k'} \pm q_{i'}|.$$

III. FORMULATION OF THE SCATTERING PROBLEM IN THE LATTICE APPROXIMATION

Now one can formulate how to solve realistic scattering problems in the wave-packet approaches. In general, we start with the f.-d. representation for the free resolvent operator [Eq. (13) or (23)] and then we derive f.-d. approximations for the scattering integral equations and all basic scattering operators.

A. Scattering wave function and the Möller wave operators

Let us apply the averaged-on-energy discretization procedure to the Lippmann-Schwinger (LS) equation for the scattering wave function:

$$|\psi_q^{L(+)}\rangle = |\psi_{0q}^{L}\rangle + g_0^{(+)}(E) v |\psi_q^{L(+)}\rangle. \tag{26}$$

By projecting the equation onto the WP basis, the following f.-d. equation for the lattice approximation $|z_k^{L(+)}\rangle$ of the wave function can be found:[7]

$$|z_k^{L(+)}\rangle = |x_k^L\rangle + \mathfrak{g}_0^{(k)} \mathfrak{v} |z_k^{L(+)}\rangle, \quad E \in [\mathcal{E}_{k-1}, \mathcal{E}_k], \tag{27}$$

where

$$\mathfrak{v} = \mathfrak{p}_L v \mathfrak{p}_L = \sum_{i,j=1}^{N} |x_i^L\rangle v_{ij} \langle x_j^L| \tag{28}$$

is the lattice approximation for the potential. The solution of Eq. (27) is assumed to be expanded on the q-packet basis:

$$|z_k^{L(+)}\rangle = \sum_{i=1}^{N} o_i^{(k)} |x_i^L\rangle. \tag{29}$$

It is clear that the expansion coefficients $o_i^{(k)}$ can be found as the the kth column of the following matrix

$$\mathbf{o}^{(k)} = \left(\mathbf{1} - \mathbf{g}_0^{(k)} \mathbf{v} \right)^{-1}. \tag{30}$$

Here and below we will use bold letters to denote matrices of corresponding operators in the lattice approximation.

It is seen from Eq. (29) that the full matrix $\mathbf{o}$ built from all these columns for $k = 1, \ldots, N$ can be recognized as the matrix of the operator:

$$\mathfrak{o} = \sum_{i=1}^{N} |z_i^{L(+)}\rangle \langle x_i^L|, \tag{31}$$

which is the nothing else but the wave-packet approximation for the Möller wave operator [27]

$$\Omega^{(+)} = \int_0^{\infty} dq\, |\psi_q^{L(+)}\rangle \langle \psi_{0q}^{L}|. \tag{32}$$

The scattering amplitude $A_L(E)$ can be found now from the well-known formula

$$A_L(E) = \frac{\mu}{q} \langle \psi_{0q}^{L} | v | \psi_q^{L(+)} \rangle, \tag{33}$$

which being rewritten in the lattice approximation takes the form

$$A_L(E) = \frac{\langle x_k^L | \mathfrak{v} | z_k^{L(+)} \rangle}{D_k}, \quad E \in [\mathcal{E}_{k-1}, \mathcal{E}_k]. \tag{34}$$

[7] We should mention that this state is not exactly the WP projection of the scattering wave function (i.e., $|z_k^{L(+)}\rangle \neq \mathfrak{p}_L |\psi_q^{L(+)}\rangle$), because $|\psi_q^{L(+)}\rangle$ is found with the complete interaction operator v, whereas the solution $|z_k^{L(+)}\rangle$ corresponds to the projected operator $\mathfrak{v}$.

In the same way, it is easy to construct fully discrete lattice analogs for all other scattering integral operators.

B. Total resolvent operator

To find the f.-d. approximation for the total resolvent operator $g(\zeta) = [\zeta - h]^{-1}$, we apply the above discretization procedure to the basic resolvent identity

$$g(\zeta) = g_0(\zeta) + g_0(\zeta) v g(\zeta),$$

which is reduced, as a result, to the f.-d. equation

$$\mathfrak{g}(\zeta) = \mathfrak{g}_0(\zeta) + \mathfrak{g}_0(\zeta)\mathfrak{v}\mathfrak{g}(\zeta), \tag{35}$$

where all the operators are projected onto the WPS. Finally, one gets the following matrix form for the lattice approximation of the total resolvent:

$$\mathbf{g}(\zeta) = [(\mathbf{g}_0(\zeta))^{-1} - \mathbf{v}]^{-1}. \tag{36}$$

It can be shown that Eq. (36) is the lattice f.-d. projection of the *exact* resolvent $\bar{g}(\zeta) = [\zeta - h_0 - \mathfrak{v}]^{-1}$, which corresponds to the Hamiltonian with the projected interaction operator $\mathfrak{v}$ (of the finite rank N) given in Eq. (28). Using formula (36), it is easy to find different types of states for the Hamiltonian with the f.-d. interaction operator $\mathfrak{v}$, viz., the bound, resonance, and continuum states. In particular, as can be seen from Eq. (36), the transcendental equation in respect of ζ

$$\det ||\mathbf{g}_0^{-1}(\zeta) - \mathbf{v}|| = 0 \tag{37}$$

determines the bound-state energies of the system when ζ is real and negative, or the resonance-state energies when ζ belongs to the nonphysical Riemann sheet. [It is straightforward to find a continuation of $\mathfrak{g}_0(\zeta)$ to this sheet using formulas (13) and (14)].

In this paper our point of interest is a scattering problem where ζ is real and positive, so in this case we will use the above average discretization procedure. Then Eq. (35) is replaced by the equation

$$\mathfrak{g}^{(k)} = \mathfrak{g}_0^{(k)} + \mathfrak{g}_0^{(k)}\mathfrak{v}\mathfrak{g}^{(k)}, \tag{38}$$

where energy $E \in [\mathcal{E}_{k-1}, \mathcal{E}_k]$ now is a completely discrete parameter. The solution of the above matrix equation is similar to Eq. (36), that is,

$$\mathbf{g}^{(k)} = \left[\left(\mathbf{g}_0^{(k)}\right)^{-1} - \mathbf{v}\right]^{-1}. \tag{39}$$

C. Energy-averaged lattice approximation for the transition operator

Consider the transition operator $t(E)$, which satisfies the LS equation

$$t(E) = v + t(E) g_0(E) v. \tag{40}$$

The off-shell t-matrix elements are usually defined as

$$t_L(q_1, q_2; E) = \frac{\mu}{\sqrt{q_1 q_2}} \langle \psi^L_{0q_1} | t(E) | \psi^L_{0q_2} \rangle. \tag{41}$$

Let us apply the energy-averaged discretization procedure to Eq. (40), which is reduced to the f.-d. analog of the LS equation:

$$\mathfrak{t}^{(k)} = \mathfrak{v} + \mathfrak{t}^{(k)}\mathfrak{g}_0^{(k)}\mathfrak{v}, \quad E \in [\mathcal{E}_{k-1}, \mathcal{E}_k], \tag{42}$$

whose explicit solutions can be written in a straightforward matrix form as

$$\mathbf{t}^{(k)} = \left[(\mathbf{v})^{-1} - \mathbf{g}_0^{(k)}\right]^{-1}. \tag{43}$$

Thus, the lattice analog for the off-shell t-matrix elements takes the form of a three-dimensional histogram [according to the projection rule of Eq. (9)]

$$t_L(q_1, q_2; E) \approx \frac{\mu\, t^{(k)}_{i_1 i_2}}{\sqrt{q^*_{i_1} d_{i_1} q^*_{i_2} d_{i_2}}}, \quad \begin{matrix} q_{1(2)} \in [q_{i_{1(2)}-1}, q_{i_{1(2)}}], \\ E \in [\mathcal{E}_{k-1}, \mathcal{E}_k], \end{matrix} \tag{44}$$

where we defined the matrix elements of the operator $\mathfrak{t}^{(k)}$ as usual

$$t^{(k)}_{ij} \equiv \langle x^L_i | \mathfrak{t}^{(k)} | x^L_j \rangle, \quad i, j = 1, \ldots, N. \tag{45}$$

The partial phase shift $\delta_L(E)$ can be extracted easily from the on-shell t-matrix element according to the well-known relation

$$-\frac{e^{i\delta_L(E)} \sin\delta_L(E)}{\pi} \approx \frac{\mu t^{(k)}_{kk}}{q^*_k d_k} \equiv \frac{t^{(k)}_{kk}}{D_k}, \quad E \in [\mathcal{E}_{k-1}, \mathcal{E}_k]. \tag{46}$$

It should be emphasized that the lattice approximated transition operators $\mathbf{t}^{(k)}$ satisfy the proper unitarity relation. Indeed, expression (43) can be rewritten in the form

$$[\mathbf{t}^{(k)}]^{-1} = \mathbf{v}^{-1} - \mathbf{g}_0^{(k)}. \tag{47}$$

Using the Hermitian conjugated equation to Eq. (47), one obtains[8]

$$\mathbf{t}^{(k)}([\mathbf{t}^{(k)}]^{-1} - [\mathbf{t}^{(k)\dagger}]^{-1})\mathbf{t}^{(k)\dagger} = \mathbf{t}^{(k)}\left(\left[\mathbf{g}_0^{(k)}\right]^\dagger - \mathbf{g}_0^{(k)}\right)\mathbf{t}^{(k)\dagger}.$$

Simplifying, one gets easily

$$\mathbf{t}^{(k)\dagger} - \mathbf{t}^{(k)} = \mathbf{t}^{(k)}\left(\left[\mathbf{g}_0^{(k)}\right]^\dagger - \mathbf{g}_0^{(k)}\right)\mathbf{t}^{(k)\dagger}. \tag{48}$$

It is clear from Eq. (48) that a discontinuity of the diagonal element of $\mathbf{t}^{(k)}$ is related to a discontinuity of the free resolvent matrix

$$\mathrm{Im} t^{(k)}_{ii} = \sum_{j=1}^{N} \mathrm{Im} g^{(k)}_j |t^{(k)}_{ji}|^2. \tag{49}$$

Then, using Eq. (25), one derives a relation between the off-shell and half-shell lattice t-matrix elements

$$\mathrm{Im} t^{(k)}_{ii} = -\frac{\pi |t^{(k)}_{ki}|^2}{D_k}. \tag{50}$$

The elastic S-matrix element is related to the above t-matrix element as

$$S^{(k)} = 1 - 2\pi \mathrm{i} \frac{t^{(k)}_{kk}}{D_k}. \tag{51}$$

Substituting Eq. (50) into the latter relation, one obtains that $|S^{(k)}| = 1$. Thus, we have just demonstrated that the S matrix defined from the lattice approximation according to

[8] For the Hermitian operator v.

Eq. (51), is *exactly unitary*. This feature is very important for practical applications and provides a stable numerical procedure.

IV. ILLUSTRATIVE EXAMPLE: LATTICE SOLUTION FOR THE SCATTERING PROBLEM WITH A NONLOCAL POTENTIAL

The WPCD method with energy-packet formalism was tested previously for many different cases of interaction potentials (local, nonlocal, energy-dependent, and complex-valued) and for the case of charged particle scattering [15–20]. It is important to stress here that the WP technique for solving scattering problems with any interaction potential is *completely universal*, i.e., the numerical procedure is the same for all types of interaction. This fact is in sharp contrast to conventional numerical routine in the coordinate space. It should be kept in mind also that the momentum-space LS equations need some special regularization procedure, since the integral kernel (i.e., the resolvent and the interaction potential) has some singularities just on the real axis. In the framework of the WP approach, all such momentum-space singularities are averaged on every bin. So the respective matrix kernels in the WP basis have a regular behavior as functions of the energy. Such an averaging will be especially important in the solution of the three- and few-body scattering problems well above the three-body threshold where the integral kernels have complicated moving singularities (see Sec. V).

As a numerical example demonstrating the advantage of the above lattice representation, we consider neutron-nucleus scattering with the optical complex-valued nonlocal potential of the Perey-Buck type [28], i.e.,

$$U(\mathbf{r},\mathbf{r}') = V\left(\tfrac{1}{2}|\mathbf{r}+\mathbf{r}'|\right)\cdot W(|\mathbf{r}-\mathbf{r}'|), \tag{52}$$

where $V(x)$ is a usual complex Woods-Saxon optical model potential of the argument $x = \frac{1}{2}|\mathbf{r}+\mathbf{r}'|$

$$V(x) = \frac{V_0}{e^{\left(\frac{x-R}{a_s}\right)}+1} + \mathrm{i}\frac{4V_d\cdot e^{\left(\frac{x-R}{a_d}\right)}}{\left[e^{\left(\frac{x-R}{a_d}\right)}+1\right]^2}, \quad R = r_0 A^{\frac{1}{3}}, \tag{53}$$

where A is the nucleus mass number, and the nonlocality W is of the Gaussian type

$$W(|\mathbf{r}-\mathbf{r}'|) = \frac{\exp[-(|\mathbf{r}-\mathbf{r}'|/\beta)^2]}{\pi^{3/2}\beta^3}, \tag{54}$$

with the scale parameter β. The potential parameter values used are $V_0 = -70$ MeV, $r_0 = 1.25$ fm, $a_s = 0.65$, $V_d = -7.0$ MeV, $a_d = 0.65$, and $\beta = 1.0$ fm for the Gaussian nonlocality. These values correspond to the neutron scattering off ^{56}Fe target [28]. For simplicity, the neutron and nucleus mass values are taken as 1 and 56 amu, correspondingly. To check the accuracy of our method, we employ a direct numerical solution of the Schrödinger equation (with the conventional Numerov method) for local phase-shift equivalent potentials (LEPs) of the Woods-Saxon type, which provide the same differential cross sections as the initial local ones at two incident neutron energies $E = 7$ and 26 MeV [28].[9]

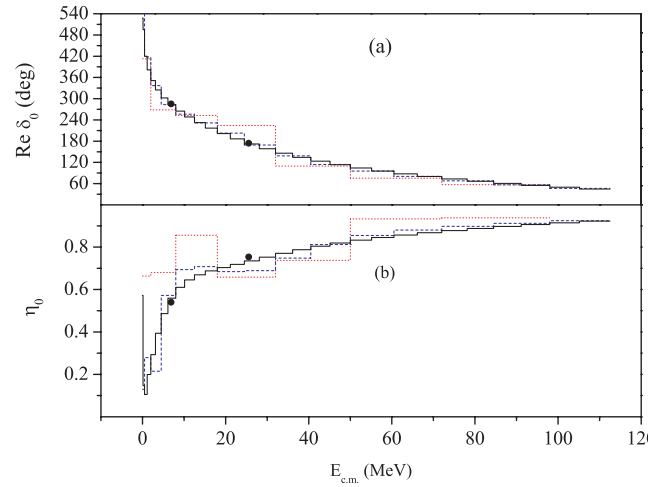

FIG. 2. (Color online) Real s-wave phase shifts Re δ_0 (top) and inelasticity parameters η_0 (bottom) for neutron scattering off ^{56}Fe (for the nonlocal optical-model potential of Perey and Buck) obtained with WPCD on the equidistant grid for different basis dimension: $N = 10$ (dotted line), $N = 20$ (dashed line), and $N = 40$ (solid line). The black circles correspond to the LEP results obtained by the direct numerical solution of the Schrödinger equation.

Two different types of bin discretization partitions were used to construct a q-packet basis for practical calculations: the equidistant (uniform) grid (EG) and the Tchebyshev grid (TG). In the EG, the maximal energy value $E_{\max}$ is fixed and the bounded area $[0, q_{\max}]$ with $q_{\max} = \sqrt{2\mu E_{\max}}$ is divided into bins of equal width d:

$$q_i = id, \quad i = 1,\ldots,N, \quad d = \frac{q_{\max}}{N}. \tag{55}$$

In Fig. 2, the s-wave real phase shifts and inelasticity parameter $\eta_0 \equiv |\exp(2i\delta_0(E))|$ with respect to increasing basis dimension N are displayed. The value $E_{\max} = 200$ MeV used in this calculation allows us to represent accurately the scattering phase shifts and inelasticity parameters in a rather wide energy range from zero energy up to 100 MeV. It is clear from the figure that despite the rather large bin width (∼10 MeV), the simple lattice-like basis with the dimension $N = 20$ is quite sufficient to obtain the converged results. Also our results nearly coincide with those for the direct numerical solution with the LEP interaction.

The TG allows us to transform a finite interval onto the $[0, \infty)$ semiaxis. The distribution has the form

$$q_i = q_{\mathrm{mid}}\left[\tan\left(\frac{2i-1}{2N}\frac{\pi}{2}\right)\right]^t, \quad i = 1,\ldots,N_L, \tag{56}$$

[9]The parameters of the LEP Woods-Saxon potentials [in notation of Eq. (53)] are $V_0 = -40.31$ MeV, $r_0 = 1.32$ fm, $a_s = 0.62$, $V_d = -3.94$ MeV, and $a_d = 0.65$ for $E = 7$ MeV; $V_0 = -34.80$ MeV, $r_0 = 1.31$ fm, $a_s = 0.62$, $V_d = -3.34$ MeV, and $a_d = 0.65$ for $E = 26$ MeV.

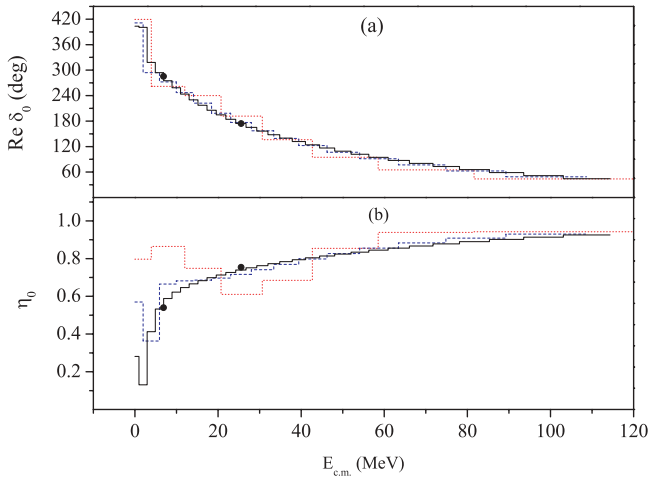

FIG. 3. (Color online) Real s-wave phase shifts Re δ_0 (top) and inelasticity parameters η_0 (bottom) for neutron scattering off ^{56}Fe with the nonlocal interaction obtained with WPCD on the Tchebyshev grid for different basis dimensions: $N = 10$ (dotted line), $N = 20$ (dashed line), and $N = 40$ (solid line). The black circles correspond to the LEP results.

where $q_{\rm mid} = \sqrt{2\mu E_{\rm mid}}$ is the common scale parameter, and the parameter t defines a spareness of the distribution (the higher t values lead to the smaller q_1 and the higher values of $q_{\rm max} \equiv q_N$). It is clear that for the TG with fixed $E_{\rm mid}$ and t values, the maximal energy is not fixed now and increases when the basis dimension N is growing. The interesting property of the TG is that its mesh points are distributed "symmetrically" in the logarithmic scale with respect to $q_{\rm mid}$, i.e.,

$$\frac{q_i}{q_{\rm mid}} = \frac{q_{\rm mid}}{q_{N-i+1}}, \quad i = 1, \ldots, N. \tag{57}$$

Thus, this distribution provides a nearly complete q-packet basis in which short-range and long-range components assist as well.

In Fig. 3, the convergence of the s-wave partial phase shifts and inelasticity parameter with increasing TG basis dimension N is given. We found that the optimal grid parameters here are $t = 0.5$ and $E_0 = 20$ MeV. As in the EG basis, dimension $N = 20$ is quite enough to provide the converged results for a wide energy interval from zero to 100 MeV.

It should be stressed that these two completely different types of discretization distribution lead to nearly coinciding results. This fact proves that the converged results of the discretization technique do not depend on the partition parameters and correspond to the initial exact scattering integral equation solution.

The structure of the TG allows us also to check the convergence with respect to the basis dimension for partial phase shifts at fixed energy E. It is convenient to use the common grid scale parameter equal to the energy value searched for, i.e., $E_{\rm mid} = E$, because the midpoint energy of the central bin (with the index $k = \frac{1}{2}N + 1$) would nearly coincide with $E_{\rm mid}$ in this case (for even N). In Table I, the S-wave phase shifts and inelasticities for different N_0 at two energies $E_{\rm lab} = 7$ and 26 MeV are given. It is obvious that the

TABLE I. Real s-wave phase shifts Re δ_0 (deg) and inelasticity parameters η_0 for neutron scattering off ^{56}Fe obtained on the Tchebyshev grid for different basis dimensions N. The LEP data correspond to direct numerical solution of the Schrödinger equation for local potentials.

N	$E_{\rm lab} = 7$ MeV		$E_{\rm lab} = 26$ MeV	
	Re δ_0	η_0	Re δ_0	η_0
10	195.56	0.561	184.64	0.682
20	285.03	0.502	175.76	0.727
40	283.28	0.529	174.07	0.741
60	284.34	0.534	173.80	0.745
80	284.90	0.534	173.71	0.745
100	285.10	0.534	173.67	0.745
LEP	285.23	0.538	174.42	0.754

q-packet method allows us to obtain the results with almost any required accuracy. The results for the LEPs are in good agreement with WPCD results found with the initial nonlocal interactions.

Finally, in Fig. 4, we display the differential cross section for the neutron scattering off ^{56}Fe at $E_{\rm lab} = 7$ MeV calculated by means of the WPCD technique with the TG of dimension $N = 100$ taken for all the partial waves (up to $L_{\rm max} = 10$) required for the convergence of the partial wave expansion. To compare, the differential cross section for the LEP is presented on the same figure. Both curves are almost indistinguishable, which proves the high accuracy of the WP technique for the nonlocal interactions.

Thus, we have demonstrated the efficiency of the wave-packet approach for the solution of the typical optical-model scattering problems with complex-valued nonlocal potentials.

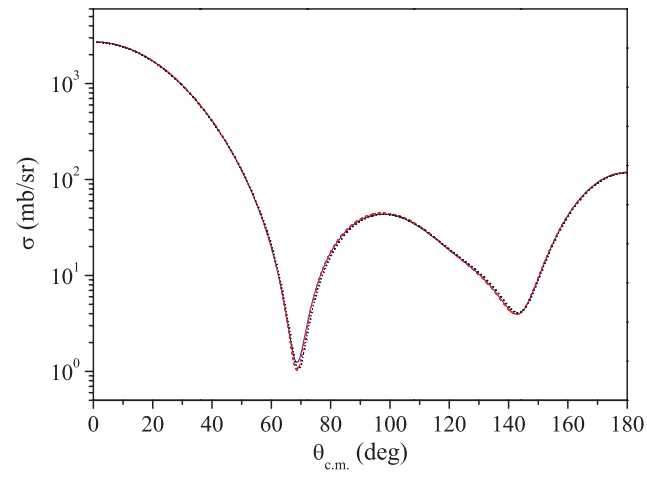

FIG. 4. (Color online) Differential cross section for neutron scattering off ^{56}Fe at $E_{\rm lab} = 7$ MeV calculated with nonlocal potential on the Tchebyshev grid with $N = 100$ (solid line) and obtained by the direct numerical solution of the Shrödinger equation with the LEP (dotted line).

V. SOLUTION OF THE THREE-BODY SCATTERING PROBLEM WITH SEPARABLE INTERACTIONS

As another nontrivial numerical illustration, we consider here the scattering problem (below and above the three-body breakup threshold) for three identical particles interacting via separable pairwise interactions. In this case (if all three particles are bosons or if they are fermions with the total spin 3/2), the Faddeev equations are reduced to a one-dimensional integral equation, which is formally similar to a two-body LS equation with a complex energy-dependent potential, the kernel of which has logarithmic singularities above the breakup threshold [29]. Thus, on the other hand, this three-body problem can be considered as a test for the extended two-body scattering problem with general complex-valued nonlocal and energy-dependent interaction potential.

To solve the three-body equations above the breakup threshold in a conventional way [29], one needs to either shift the path of integration into the complex momentum plane (where the kernel becomes regular) or solve the equation at complex energies and then continue analytically the solution to the real energy axis [30]. Below we will demonstrate that the lattice representation approach allows us to replace such an equation with a corresponding matrix equation and to solve it immediately on the real energy axis without any deformation of the path of integration.

A. Definitions

We consider the system of three identical particles with mass m interacting by means of the separable potential

$$v = \lambda|\varphi\rangle\langle\varphi|. \tag{58}$$

the two-body t matrix for such a potential has also a separable form

$$t(E) = |\varphi\rangle\tau(E)\langle\varphi|, \tag{59}$$

where

$$\tau^{-1}(E) = \lambda^{-1} - J(E) \equiv \lambda^{-1} - \langle\varphi|g_0(E)|\varphi\rangle, \tag{60}$$

and $g_0(E)$ is the free two-particle resolvent. If a bound state with energy $E_b < 0$ exists (and we consider just this case), then the binding energy E_b defined by the equation $\lambda^{-1} = J(E_b)$ is a convenient parameter replacing λ.

The function $\tau(E)$ is the analytical function with a single pole at $E = E_b$, and its residue at this pole, $R(E_b)$, being equal to

$$R(E_b) = -\left[\frac{dJ}{dE}\right]_{E=E_b}^{-1}, \tag{61}$$

defines the normalization of the bound-state wave function $|\psi_b\rangle$ as

$$|\psi_b\rangle = \sqrt{R(E_b)}g_0(E_b)|\varphi\rangle. \tag{62}$$

More definitely we will use the two-parameter Yamaguchi potential with the form factor:

$$\langle\mathbf{p}|\varphi\rangle \equiv \varphi(\mathbf{p}) = (p^2 + \beta^2)^{-1}. \tag{63}$$

In this case, one gets the following explicit formulas for $\tau(E)$ and $R(E_b)$:

$$\begin{aligned}\tau^{-1}(E > 0) &= -\frac{\pi^2 m}{\beta}\left(\frac{1}{(\beta + p_b)^2} - \frac{1}{(\beta - ip)^2}\right),\\ p &= \sqrt{mE}, \quad p_b = \sqrt{-mE_b},\\ R(E_b) &= \frac{\beta\left(b^2 + p_b^2\right)^3 p_b}{\pi^2 m}.\end{aligned} \tag{64}$$

The elastic scattering amplitude $2 \to 2$ can be found, as is well known [29], from the Faddeev integral equation for the function $F(\mathbf{q}, \mathbf{q}'; E) \equiv \langle\mathbf{q}, \varphi|g_0(E)U(E)g_0(E)|\mathbf{q}', \varphi\rangle$, where U is the transition operator,

$$\begin{aligned}F(\mathbf{q}, \mathbf{q}'; E) = 2Z(\mathbf{q}, \mathbf{q}'; E) + 2\int Z(\mathbf{q}', \mathbf{q}''; E)\\ \times \tau\left(E - \frac{3(\mathbf{q}'')^2}{4m}\right) F(\mathbf{q}'', \mathbf{q}'; E)\, d^3q''.\end{aligned} \tag{65}$$

So the on-shell amplitude can be defined from the relation

$$\begin{aligned}A(E, \cos\theta) &= R(E_b)F(\mathbf{q_0}, \mathbf{q_0'}; E),\\ q_0 = q_0' &= \sqrt{\frac{4}{3}m(E - E_b)}, \quad \cos\theta = \frac{\mathbf{q_0}\cdot\mathbf{q_0'}}{q_0 q_0'},\end{aligned} \tag{66}$$

where $\mathbf{q_0}$ and $\mathbf{q_0'}$ are the initial and final c.m. momenta.

The factors of 2 in Eq. (65) correspond to the case of three identical bosons; while for three fermions in quartet spin channel, these factors should be replaced by -1. The kernel function $Z(\mathbf{q}, \mathbf{q}'; E)$ in Eq. (65) is defined as

$$Z(\mathbf{q}, \mathbf{q}'; E) = \frac{\varphi(\mathbf{q}' + \mathbf{q}/2)\varphi(-\mathbf{q} - \mathbf{q}'/2)}{E - q^2/m - q'^2/m - qq'/m}. \tag{67}$$

After the partial-wave expansion of the functions F and Z in Eq. (65), one gets the one-dimensional integral Faddeev equation in the Lth partial wave

$$\begin{aligned}F_L(q, q'; E) = 2Z_L(q, q'; E) + 2\times 4\pi\int Z_L(q', q''; E)\\ \times \tau\left(E - \frac{3(q'')^2}{4m}\right) F_L(q'', q'; E)(q'')^2 dq'',\end{aligned} \tag{68}$$

which takes the form of the two-body LS equation in which $Z_L(E)$ can be considered as the effective E-dependent potential, and the function $\tau(E - 3q^2/4m)$ plays the role of the free resolvent.

For the Yamaguchi potential, one gets an explicit formula for the kernel function Z_L. The function is regular at $E < 0$ and has the logarithmic singularities at $E > 0$. In s-wave scattering, the singular part of Z_0 takes the form [29]

$$\begin{aligned}Z_0^{\text{sing}}(q, q'; E) = \frac{m}{qq'}\frac{1}{\left(Em + \beta^2 - \frac{3}{4}q^2\right)\left(Em + \beta^2 - \frac{3}{4}q'^2\right)}\\ \times \ln\frac{\left(Em - \frac{3}{4}q^2\right) - (q' + q/2)^2}{\left(Em - \frac{3}{4}q^2\right) - (q' - q/2)^2}.\end{aligned} \tag{69}$$

Note that the singular part of Z_0 for any form factor φ is proportional to the same logarithm as in Eq. (69).

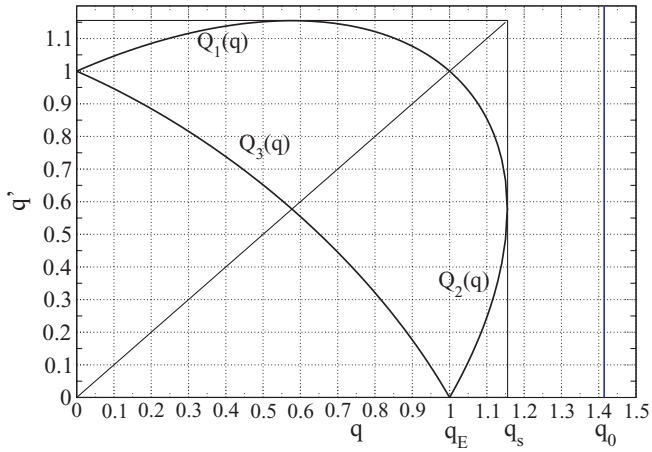

FIG. 5. (Color online) Part of the (q, q') plane where the singularities of the Faddeev kernel of Eq. (68) for $q_E = \sqrt{Em} = 1$ are located. The logarithmic singularities of Z_0 lie on the elliptic arcs $Q_1(q)$, $Q_2(q)$, $Q_3(q)$; the region Ω where the imaginary part of Z_0 is different from zero is between these arcs and inside the rectangle $(q, q') < q_s = \sqrt{\frac{4}{3}}q_E$. The vertical line at $q = q_0$ corresponds to the pole of the "propagator" $\tau(E - 3q^2/4m)$ for $mE_b = -0.5$. The grid lines reflect the lattice discretization cells.

The area of singularities for the kernel of the integral equation (68) is shown in Fig. 5. The factor $\tau(E - 3q^2/4m)$ as a function of q has a simple pole at $q = q_0 = \sqrt{\frac{4}{3}m(E - E_b)}$ (for any energy $E > E_b$). The position of singularities of Z_0 is determined by zeros of the numerator and denominator under the logarithm symbol in Eq. (69). Above the three-body breakup threshold ($E > 0$), we introduce two values of momentum: $q_E = \sqrt{Em}$ and $q_s = \sqrt{\frac{4}{3}}q_E$. From Eq. (69) it is obvious that there are no singularities of Z_0 when $q > q_s$ or $q' > q_s$, otherwise the singularities lie on the arcs of two ellipses (Q_1, Q_2) and Q_3 (see Fig. 5), the imaginary part of Z_0 being different from zero only in the region Ω between these two arcs.

So, it is clear that the direct numerical solution of Eq. (68) is not a simple problem on the positive real axis of q due to the noted singularities of the kernel. However, the application of the lattice approximation leads to the discretization of q and q' variables and averaging of Z_0 and τ functions over the cells of the constructed lattice in the (q, q') plane, i.e., to some effective regularization of the kernel in Eq. (68).

B. Lattice approximated solution

The discretization procedure (defined in Sec. II C) being applied to the Faddeev equation (68) results directly in its matrix analog

$$\mathbf{F}(E) = 2\mathbf{Z}(E) + 2 \times 4\pi \mathbf{Z}(E)\boldsymbol{\tau}(E)\mathbf{F}(E). \tag{70}$$

Here we use the basis of s-wave q packets $|x_i^0\rangle$ defined in Eq. (3), so that the matrix elements in Eq. (70) are equal, i.e.,

$$Z_{ij}(E) = \langle x_i^0 | Z_0 | x_j^0 \rangle = \frac{1}{\sqrt{d_i d_j}} \int_{q_{i-1}}^{q_i} \int_{q_{j-1}}^{q_j} Z_0(q, q'; E) dq\, dq', \tag{71}$$

and $\boldsymbol{\tau}$ is the diagonal matrix with elements

$$\tau_i(E) = \frac{1}{d_i} \int_{q_{i-1}}^{q_i} \tau\left(E - \frac{q^2}{4m/3}\right) dq. \tag{72}$$

The matrix elements in Eq. (72) can be replaced by values of τ calculated in the midpoints q_i^* of the ith interval. So, we can use the following approximation for $\tau_i(E)$:

$$\tau_i(E) \simeq \tilde{\tau}_i(E) = \begin{cases} \tau(E - 3q_i^{*2}/4m), & i \neq k, \\ -\dfrac{i\pi}{d_k}\dfrac{2m}{3q_0} R_b(E_b), & i = k, \end{cases} \tag{73}$$

where index k denotes the "singular" interval to which the pole of the function $\tau(q) = \tau(E - 3q_i^2/4m)$ belongs. However, to check carefully the quality of this midpoint approximation (73), we also calculated the same matrix elements directly by applying the 48-point Gaussian quadrature on each bin, taking into account the possible singularity of the integrands. The comparison between the exact values for the matrix elements τ_i and their approximated values $\tilde{\tau}_i$ is shown in Fig. 6. From the figure it is evident that the midpoint approximation gives very accurate representation for all matrix elements (bin projections) of $\tau_i(E)$.

Regarding the matrix elements Z_{ij}, one has to keep in mind that the singularities of the integrand $Z_0(q, q', E)$ are logarithmic, so they can be integrated in common sense. Thus, the following simple approximation can be used for all intervals:

$$\mathrm{Re}\, Z_{ij}(E) \approx \mathrm{Re}\, \tilde{Z}_{ij}(E) = \mathrm{Re}\, Z_0(q_i^*, q_j^*; E)\sqrt{d_i d_j}. \tag{74}$$

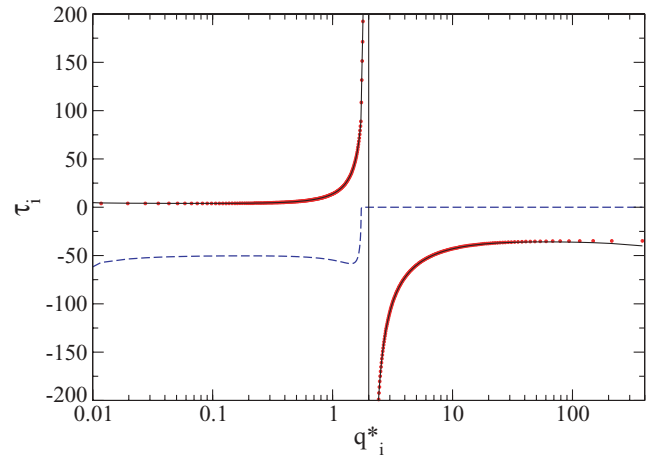

FIG. 6. (Color online) Comparison between the midpoint values $\tilde{\tau}_i$ (circles) and exact matrix elements τ_i (solid line) considered as functions of midpoint momentum q_i^*. The imaginary part of τ_i is shown by the dashed line. The difference between exact and midpoint values for the imaginary part is almost invisible.

$$\mathrm{Im}\tilde{Z}_{ij}(E) = \begin{cases} -\dfrac{\pi m}{q_i^* q_j^*} \dfrac{\sqrt{d_i d_j}}{\left(Em + \beta^2 - \frac{3}{4}q_i^{*2}\right)\left(Em + \beta^2 - \frac{3}{4}q_j^{*2}\right)}, & (q_i^*, q_j^*) \in \Omega, \\ 0, & (q_i^*, q_j^*) \in \Omega, \end{cases} \tag{75}$$

which is nonzero for the lattice cells that belong to the region Ω. In fact, such an approximation means a replacement of the smooth boundary (the arcs) for the Ω region by the step-like one. The comparison between the exact diagonal matrix elements Z_{ii} and approximate ones [given by Eqs. (74) and (75)] calculated at $E = 30$ (in units $2m = 1$) when choosing $N = 200$ equidistant momentum bins is shown in Fig. 7. A similar accuracy is reached also for the nondiagonal matrix elements $Z_{ij}(E)$.

Thus it is evident from the above comparisons that the construction of f.-d. matrix kernel on the q-packet basis can be done immediately and in a very simple way just on the real axis (i.e., without any contour deformation).

C. Calculations of phase shifts and inelasticity parameters

After having solved Eq. (70), the complex partial phase shift for an elastic $2 \to 2$ scattering can be found from the relation

$$e^{2i\delta_0(E)} = 1 - 2\pi i \frac{2m}{3q_0 d_k} R_B(E_B) F_{kk}(E), \quad q_0 \in [q_{k-1}, q_k]. \tag{76}$$

In Figs. 8 and 9, we present the energy dependence of the real phase shift $\delta(E)$ and the inelasticity parameter $\eta(E)$ obtained from our lattice calculations [solution of the matrix equation (70)] for the elastic s-wave scattering in the three-boson system. In this illustrative calculation, the Yamaguchi potential parameters $2m = 1$, $E_b = -1.5$, $\beta = 5$ were used. The calculations were carried out with the approximate values for matrix elements (73)–(75) found with the simple midpoint way. This allowed us to reduce the computational effort and time enormously (by one to two orders of magnitude).

As is well known [29], the main difficulty in performing the Faddeev three-body calculations above the breakup threshold in momentum space is the appearance of moving singularities in the integral kernel Z_0 at $E > 0$, which correspond to three-body breakup of the system. To describe properly these singularities, it is necessary to cover the whole region Ω in the (q, q') plane [i.e., the rectangle $(q, q') < q_s$] by the sufficiently dense lattice. Therefore, to optimize the numeric treatment, we used a combined grid for different q intervals: the EG: $q_i = q_s(i/N_1)$, $i = 1, \ldots, N_1$ was used in the "singular" region $0 < q < q_s$; and the TG: $q_i = q_0[\tan(\frac{2i-1}{2N_2}\frac{\pi}{2})]$, $i = 1, \ldots, N_2$ turned out to be preferable[10] in the regular region $q > q_s$.

To check the reliability and accuracy of our approach, we compared the s-wave phase shifts and inelasticity parameters for the quartet nd scattering (with the Yamaguchi pairwise potential) obtained in the WP approach with the respective results obtained by the conventional approaches [31,32] to the

[10]This choice is related to the fact that TG is more suitable for the high momenta region than EG, because the Tchebyshev distribution (58) of a rather small dimension (being constructed to transform a finite interval onto an infinite one) contains intermediate and very high momenta values as well.

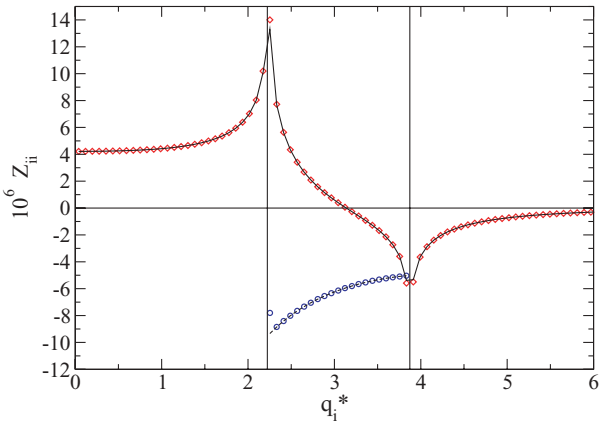

FIG. 7. (Color online) Diagonal matrix element Z_{ii} as function of midpoint momentum q_i^* for the uniform EG with the width value $d = 0.079$ and $E = 30$. The exact integrals over momentum bins (real part, diamonds; imaginary part, circles) are compared with their midpoint approximations (real part, solid line; imaginary part, dashed line). The vertical lines correspond to positions of the logarithmic singularities of the initial function $Z_0(q_i^*, q_i^*, E)$.

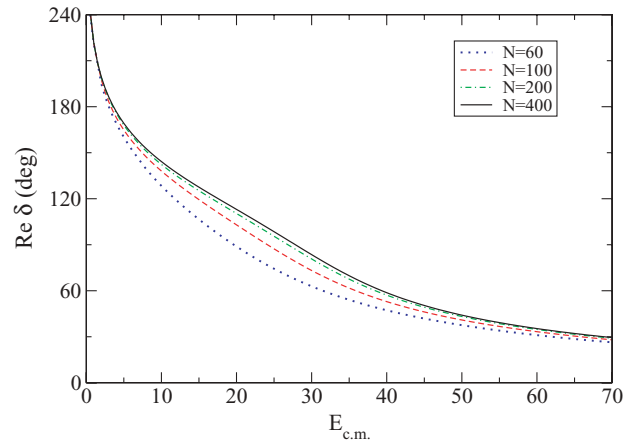

FIG. 8. (Color online) Energy dependence of the real s-wave phase shift for the elastic $2 \to 2$ scattering in the model three-identical-boson system calculated by means of the momentum-packet discretized Faddeev equation (70) for different dimensions $N = 60$–400 of the wave-packet basis. The model parameters are $2m = 1$, $E_b = -1.5$, $\beta = 5$.

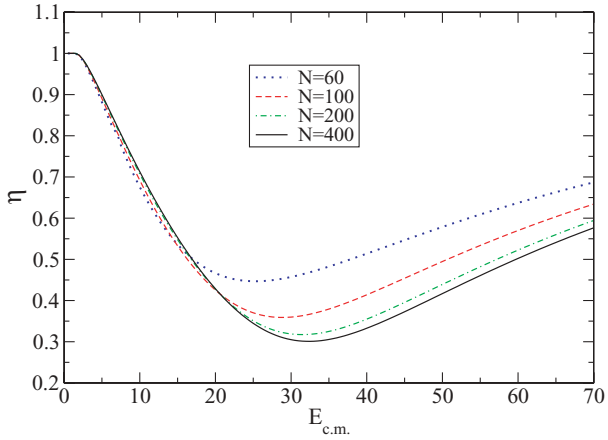

FIG. 9. (Color online) Same as in Fig. 8, but for the inelasticity parameter.

numerical solution of Eq. (65). In the Table II, we present the convergence of our wave-packet results and data from Ref. [31] at three energies: $E_{\rm lab} = 0.5$, 14.1, and 50 MeV. The parameters of the Yamaguchi potential were chosen to be the same as in Ref. [31] (they were fitted to the values of the deuteron binding energy $E_b = -2.226$ MeV and the triplet scattering length $a_t = 5.41$ fm). The value of $\hbar^2/m$ is equal to 41.4594 MeV fm^2.

Thus, one can see from Figs. 8 and 9 and Table II that the wave-packet discretization method with momentum lattice allows one to solve the Faddeev equations *above the three-body threshold* straightforwardly at real energy, i.e., without any contour deformation. It simplifies drastically the whole solution algorithm. The proper analytical behavior of the discretized (matrix) kernel in Eq. (70) is ensured in this case by the fact that we employed in our lattice discretization the matrix elements of the exact function Z_0 which includes explicitly all the singularities of the initial integral kernel. For local (or arbitrary nonlocal) pairwise interactions, it would seem that the most economic and straightforward way is to use a separable expansion of the input interaction (just as it was done in numerous previous works) and then to apply the above direct lattice discretization (with a trivial extension) to the resulting one-dimensional integral equations.

However, we found that it is much more advantageous in the general case to employ another way for the solution, namely, *the direct lattice discretization* of two-dimensional three-body integral equations (Faddeev or Lippmann-Schwinger) and three-dimensional four-body Yakubovsky equations using the respective two- or three-dimensional momentum-packet bases along two or three Jacobi coordinates (i.e., the two- or three-dimensional lattice; see the next section).

TABLE II. Comparison of our wave-packet real phase shifts Re δ (deg) and inelasticity parameters η with those calculated by Sloan [31] and by Larson and Hetherington [32] for s-wave quartet nd scattering with the Yamaguchi pairwise potential at three energies.

N	$E_{\rm lab} = 0.5$ MeV[a] Re δ	$E_{\rm lab} = 14.1$ MeV		$E_{\rm lab} = 50$ MeV	
		Re δ	η	Re δ	η
48	144.83	71.9	1.035	39.1	0.923
96	145.92	72.9	0.998	37.7	0.909
192	145.04	72.5	0.985	37.2	0.889
512	145.08	72.1	0.980	37.1	0.885
1024	145.10	72.0	0.978	37.1	0.884
Ref. [31]	145.1	71.9	0.978	37.0	0.884
Ref. [32]	145.1	71.9	0.975	36.9	0.891

[a]At this energy, $\eta = 1.0$.

VI. SOLUTION OF THE GENERAL THREE-BODY SCATTERING PROBLEM

Here we will briefly describe how the wave-packet technique can be applied to the general three- or few-body scattering problem with any type of interaction potential including local, nonlocal, etc., ones by introducing the two-dimensional momentum lattice.

A. Lattice representation for the channel resolvent

Let us consider the general three-body scattering problem for particles 1, 2 and 3, interacting via pair short-range potentials v_i $(i = 1, 2, 3)$. It is convenient to use three Jacobi coordinate sets corresponding to three channel Hamiltonians H_i $(i = 1, 2, 3)$ which define asymptotic motions in the system. In the general case, the respective wave-packet basis should be constructed independently for each Jacobi set [18].

The channel Hamiltonian H_1 has the form of the direct sum of the two-body sub-Hamiltonians

$$H_1 \equiv h_1 \oplus h_0^1, \tag{77}$$

where sub-Hamiltonian h_1 defines the interaction in the {23} subsystem (i.e., including the potential v_1), and the sub-Hamiltonian h_0^1 corresponds to the free relative motion of this subsystem (its center of mass) and the spectator particle 1. The eigenfunction of the three-body Hamiltonian H_1 corresponding to the given value of the total angular momentum Λ and its projection $\mathcal{M}$ can be written in the form

$$\langle \mathbf{p}', \mathbf{q}' | \psi_p^l, \psi_{0q}^L, \Lambda\mathcal{M}\rangle \equiv \psi_p^l(p')\psi_{0q}^L(q')\mathcal{Y}_{lL}^{\Lambda\mathcal{M}}(\hat{\mathbf{p}}', \hat{\mathbf{q}}'), \tag{78}$$

where $\mathbf{p}'$ and $\mathbf{q}'$ are the relative and c.m. Jacobi momenta; $\psi_p^l(p')$ and $\psi_{0q}^L(q')$ are the radial wave functions corresponding to the sub-Hamiltonians h_1 and h_0^1 with angular momenta $\mathbf{l}$ and $\mathbf{L}$, respectively. The $\mathcal{Y}_{lL}^{\Lambda\mathcal{M}}(\hat{\mathbf{p}}', \hat{\mathbf{q}}')$ are six-dimensional spherical harmonics given by the convolution of the spherical functions $Y_{l\mu_1}(\hat{\mathbf{p}}')$ and $Y_{L\mu_2}(\hat{\mathbf{q}}')$.

Now we introduce the WP bases for two-body sub-Hamiltonians h_1 and h_0^1. Assume further that there are K_b^l bound states (for a fixed partial wave l) in the {23} subsystem with corresponding bound-state wave functions $\{|z_n^l\rangle\}_{n=1}^{K_b^l}$ and eigenenergies $\{\epsilon_n^{l*}\}_{n=1}^{K_b^l}$. Let us define the partition $[\epsilon_{i-1}^l, \epsilon_i^l]_{i=K_b^l+1}^{K^l}$ of the continuous spectrum of h_1 (with corresponding momentum bins $[p_{i-1}^l, p_i^l]_{i=K_b^l+1}^{K_l}$) and construct

the set of scattering wave packets from the respective exact scattering wave functions $|\psi_p^l\rangle$ [similar to Eq. (3)]:

$$|z_i^l\rangle = \frac{1}{\sqrt{A_i^l}} \int_{p_{i-1}^l}^{p_i^l} \mathrm{d}p\, w(p) |\psi_p^l\rangle, \tag{79}$$

where A_i^l and $w(p)$ are normalization factors and the weight function, respectively. The full lattice basis $\{|z_i^l\rangle\}_{i=1}^{K_l}$ for the h_1 sub-Hamiltonian includes the bound-state functions and the scattering wave packets. Free wave packets [Eq. (3)] corresponding to the h_0^1 sub-Hamiltonian are constructed with the use of the partition $[q_{j-1}^L, q_j^L]_{j=1}^{N_L}$ in the continuous spectrum of the h_0^1.

Now one can build the three-body wave-packets (3WP) just as products of two types of wave-packet states (for the above two sub-Hamiltonians) whose angular parts are combined with the total angular momentum value Λ as in Eq. (78):

$$|Z_S^{\Lambda\mathcal{M}}\rangle \equiv |z_i^l, x_j^L, \Lambda\mathcal{M}\rangle, \; i = 1, \ldots, K_l, \quad j = 1, \ldots, N_L, \tag{80}$$

where $S = i, l, j, L$ is the multi-index. Further, we will omit the index $\mathcal{M}$. The properties of the 3WP constructed in this way are the same as those of the two-body wave packets, *viz.*, they form an orthonormal set, and any operator functionally dependent of the channel Hamiltonian H_1 has the diagonal projection onto the subspace spanned on this basis. It allows us to construct an analytical f.-d. approximation for the three-body channel resolvent $G_1(E) \equiv [E + \mathrm{i}0 - H_1]^{-1}$.

Indeed, the exact three-body channel resolvent is the convolution of the two-body subresolvents $g_1(E)$ and $g_0(E)$:

$$G_1(E) = \frac{1}{2\pi \mathrm{i}} \int_{-\infty}^{\infty} d\epsilon\, g_1(\epsilon) g_0(E - \epsilon). \tag{81}$$

Using spectral expansions for the two-body resolvents and performing the integration, one gets an explicit expression for the exact channel resolvent G_1 as a sum of two terms $G_1(E) = G_1^{\mathrm{BC}}(E) + G_1^{\mathrm{CC}}$, where the bound-continuum part takes the form

$$G_1^{\mathrm{BC}}(E) = \sum_{l,L} \sum_{n=1}^{K_b^l} \int_0^{\infty} dq \frac{|z_n^l, \psi_{0q}^L, \Lambda\rangle\langle z_n^l, \psi_{0q}^L, \Lambda|}{E + \mathrm{i}0 - \epsilon_n^{l*} - \frac{q^2}{2M}}, \tag{82}$$

where M is the reduced mass in the $\{23\} + 1$ channel. The continuum-continuum part of G_1 takes the form

$$G_1^{\mathrm{CC}}(E) = \sum_{l,L} \int_0^{\infty} dp \int_0^{\infty} dq \frac{|\psi_p^l, \psi_{0q}^L, \Lambda\rangle\langle \psi_p^l, \psi_{0q}^L, \Lambda|}{E + \mathrm{i}0 - \frac{p^2}{2\mu} - \frac{q^2}{2M}}, \tag{83}$$

where μ is the reduced mass in the $\{23\}$ subsystem.

Projecting further the exact channel resolvent onto 3WP basis defined in Eq. (80), one can find the following analytical formulas for the diagonal f.-d. approximation of the G_1 operator:

$$\begin{aligned} \mathfrak{G}_1^{\mathrm{BC}} &= \sum_{l,L} \sum_{n=1}^{K_b^l} \sum_{j=1}^{N_L} G_{nljL}^{\mathrm{BC}} |z_n^l, x_j^L, \Lambda\rangle\langle z_n^l, x_j^L, \Lambda|, \\ \mathfrak{G}_1^{\mathrm{CC}} &= \sum_{i=K_b^l+1}^{K_l} \sum_{j=1}^{N_L} G_{iljL}^{\mathrm{CC}} |z_i^l, x_j^L, \Lambda\rangle\langle z_i^l, x_j^L, \Lambda|, \end{aligned} \tag{84}$$

where the matrix elements G_{nljL}^{BC} and G_{iljL}^{CC} are defined as integrals over the respective momentum bins:

$$G_{nljL}^{\mathrm{BC}} = \frac{1}{B_j^L} \int_{q_{j-1}^L}^{q_j^L} \frac{|f(q)|^2 dq}{E + \mathrm{i}0 - \epsilon_n^{l*} - \frac{q^2}{2M}}, \tag{84a}$$

$$G_{iljL}^{\mathrm{CC}} = \frac{1}{A_i^l B_j^L} \int_{p_{i-1}^l}^{p_i^l} \int_{q_{j-1}^L}^{q_j^L} \frac{|w(p)|^2 |f(q)|^2 dp\, dq}{E + \mathrm{i}0 - \frac{p^2}{2\mu} - \frac{q^2}{2M}}. \tag{84b}$$

These matrix elements depend, in general, on the spectrum partition parameters (i.e., p_i^l and q_j^L values) and the total energy only and do not depend explicitly on the interaction potential v_1. When the wave-packet expansions of the three-body amplitude is convergent, the final result turns out to be *independent* upon the particular spectral partition parameters. The integrals in Eqs. (84) and can be taken in a closed form, which gives a convenient analytical f.-d. representation for the three-body channel resolvent G_1. We have calculated these matrix elements for the case of energy packets (the explicit formulas can be found in Ref. [18]).

The representation (84) for the channel resolvent is a basic feature of the wave-packet approach since it allows us to drastically simplify the solution of the general three-body scattering problem. In particular, this representation has been used to solve the f.-d. analog for the Faddeev equations for the Faddeev components of the total scattering wave function [18]. Alternatively, this representation has been used also to solve some particular three-body scattering problems with employment of the three- or few-body Lippmann-Schwinger equations [19,20], e.g., for composite projectile scattering off a nuclear target (see below) or for electron-atom and electron-molecule scattering above the first ionization threshold, etc.[11]

B. Application to solving three-body integral equations with noncompact kernels

To illustrate the effectiveness of the lattice approximation in the three-body scattering problem, we consider here the scattering of composite two-fragment particle {23} off a heavy target-nucleus 1. For simplicity, we assume that the fragments have equal masses and there is only one s-wave bound state $|z_1^0\rangle$ with the binding energy ϵ_1^{0*} in the {23} subsystem.

[11] The WP technique for the two-body Coulomb interaction is given in Ref. [17]. The generalization of the approach to the few-body scattering problems with charged particles will be considered in our next paper.

In the conventional treatment, the system Hamiltonian can be written in the form [22]

$$H = H_1 + v_2 + v_3, \tag{85}$$

where H_1 is the channel Hamiltonian defined in Eq. (77),[12] and $v_{2(3)}$ are optical-model potentials of fragment-target interactions.

Since there are no bound states in each projectile fragment-target subsystem due to the complex optical-model interactions, the total scattering wave function can be uniquely found from the *single* three-body Lippmann-Schwinger equation (according to Ref. [22])

$$|\Psi^{\Lambda}(E)\rangle = \left|\Psi_1^{\Lambda}(E)\right\rangle + G_1(E)\bar{V}_1|\Psi^{\Lambda}(E)\rangle, \tag{86}$$

where $\bar{V}_1 \equiv v_2 + v_3$ is the "external" interaction, and $|\Psi_1^{\Lambda}(E)\rangle \equiv |z_1^0, \psi_{0q_0}^{\Lambda}, \Lambda\rangle$ is the outgoing wave function for the projectile in its bound state. The on-shell momenta is defined as $q_0 = \sqrt{2M(E - \epsilon_1^{0*})}$.

The main problem with solution of Eq. (86) is that its kernel is noncompact [22] (so it has no finite Hilbert-Schmidt norm) and includes a δ function. So the direct numerical solution requires some nontrivial special numerical techniques for solving singular equations. In practice, most of authors prefer to use a coupled-channel method (on the base of the Schrödinger differential equation) to find the elastic and breakup scattering amplitudes. On the contrary, in the wave-packet approach, we can use just the integral equation framework (86) because there is no problem with the compactness of the three-body kernel in Eq. (86).[13] We apply the discretization procedure to this equation using the 3WP basis corresponding to the channel Hamiltonian H_1. After this discretization, the integral equation (86) takes the f.-d. form

$$|\hat{\Psi}^{\Lambda}(E)\rangle = \left|Z_{S_0}^{\Lambda}\right\rangle + \mathfrak{G}_1(E)\mathfrak{V}|\hat{\Psi}^{\Lambda}(E)\rangle, \tag{87}$$

where $|Z_{S_0}^{\Lambda}\rangle \equiv |z_1^0, x_{k_0}^{\Lambda}, \Lambda\rangle$ is the wave-packet state corresponding to the initial wave function $|\Psi_1^{\Lambda}\rangle$ (the index k_0 being defined by the energy conservation rule: $E \in [\mathcal{E}_{k_0-1}^{\Lambda} + \epsilon_1^{0*}, \mathcal{E}_{k_0}^{\Lambda} + \epsilon_1^{0*}]$), and the wave packet projection of the channel resolvent $\mathfrak{G}_1$ is calculated by the explicit formulas (84). The external interaction $\mathfrak{V}$ can be found here in the matrix form

$$\mathfrak{V} \equiv \sum_{S,S'} \left|Z_S^{\Lambda}\right\rangle V_{S,S'} \left\langle Z_{S'}^{\Lambda}\right|, \tag{88}$$

where the matrix elements $V_{S,S'} \equiv \langle z_i^0, x_j^{\Lambda}, \Lambda|v_2 + v_3|z_{i'}^0, x_{j'}^{\Lambda}, \Lambda\rangle$ *are* calculated in the lattice basis analytically or numerically.

It was shown previously [18–20] that the interaction wave packets $|z_i^0\rangle$ jointly with the bound-state function $|z_1^0\rangle$ can be approximated with very high accuracy by variational functions obtained from the diagonalization of the sub-Hamiltonian h_1 in some L_2 basis $\{|\phi_n\rangle\}$. So, they can be represented by the following expansions in the chosen basis:

$$\left|z_i^0\right\rangle = \sum_{n=1}^{K} O_{in}|\phi_n\rangle, \quad i = 1, \ldots, K_0. \tag{89}$$

In the calculations presented here, the Gaussian bases have been used in the expansion (93). However in the general three-body scattering problem (including the rearrangement channels), the basis of exact free q packets is more preferable for diagonalization of the sub-Hamiltonian h_1.

Finally, the elastic scattering amplitude is determined formally by the expression

$$A_{\mathrm{el}}^{\Lambda} \approx \frac{[(\mathbf{V}^{-1} - \mathbf{G}_1)^{-1}]_{S_0,S_0}}{D_{k_0}^{\Lambda}}, \tag{90}$$

where the bold letters denote matrices of the respective operators in 3WP basis and $D_{k_0}^{\Lambda}$ is the bin width of the h_0^1 continuous spectrum discretization. It should be emphasized here that the three-body breakup amplitude can be found immediately as a nondiagonal (off-shell) matrix element of *the same matrix* $[\mathbf{V}^{-1} - \mathbf{G}_1]^{-1}$ in the 3WP basis [18,20]. The above matrix is in essence a finite-dimensional analog of the exact transition operator.

It is important to note that the above integral formulation of the initial three-body scattering problem has evident advantages over the coupled-channel differential approaches (i.e., those based on the Schrödinger equation formulation) traditionally used for solving such problems. Consider, for example, the CDCC method [15,21–24], which is based on the discretization of the {23} subsystem internal continuum only. This partial discretization procedure allows one to reduce the initial three-body Schrödinger equation to the two-body coupled-channel problem still in differential equation framework in which matching with asymptotic outgoing waves are taken along the center-of-mass coordinate only. However, in the integral WPCD approach, the outgoing boundary conditions along *both* Jacobi coordinates are considered *symmetrically* owing to the proper approximation for the channel resolvent. Moreover, the closed channels of the {23} subsystem are included into the integral WPCD scheme in the same way as the opened ones, while in the CDCC the direct inclusion of

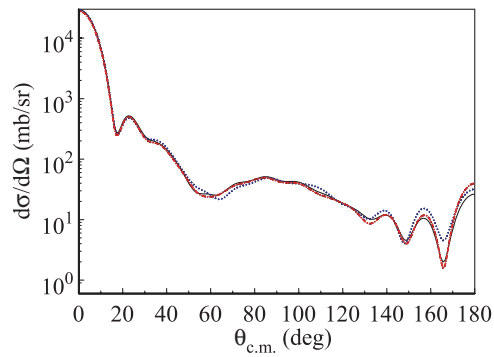

FIG. 10. (Color online) Differential cross section for the FVA model calculated within the CDCC (dotted curve), the FEM (dash-dotted curve), and the lattice approximation (solid curve) methods.

[12]We neglect here for simplicity the Coulomb interaction, but in its presence the lattice formalism remains in principle the same (see Refs. [15,20]).

[13]In this case, the δ function singularity in the kernel is integrated (smeared) over the respective bin and gives a finite contribution to the matrix element of the kernel.

the closed-channel effect leads to numerical instabilities, and a special R-matrix coupled-channel technique [24] is required in this case. Finally, thanks to the integral formulation of the problem, the WPCD scheme can be generalized directly to include the rearrangement (e.g., the stripping, etc.) channels in the system, while in the CDCC scheme such generalization is rather nontrivial.

The detailed comparison between two methods of the continuum discretization has been discussed in Ref. [15]. In the present work, we compare for illustrative purposes in Fig. 10 the differential cross sections for the Farell-Vincent-Austern (FVA) model [21,22] (traditionally used as a test for the composite particle scattering problem) calculated within the WPCD and CDCC approaches. As an independent test, we display here the results of the direct solution of the three-body Schrödinger equation with proper three-body boundary conditions found in Ref. [22] within the finite element method (FEM). It is clear from Fig. 10 that the WPCD and FEM results are very close to each other, while the CDCC result differs a little bit from them at backward angles. These discrepancies are very likely related to fact that FEM and WPCD approaches both include accurately the closed-channel contributions, which are neglected in the CDCC framework.

C. Application to the general Faddeev equations

When rearrangement channels cannot be neglected, the general Faddeev formalism should be used to solve the full three-body scattering problem of $2 \to 2$ or $2 \to 3$ type. So, in the Faddeev approach, we introduce three sets of 3WPs $\{Z_S^{(a)}\}$, $a = 1, 2, 3$, related to three channel Hamiltonians H_a.[14] Further, we apply the complete discretization procedure directly to the system of three Faddeev equations (e.g., for the wave function with the initial state $|\Phi_{01}\rangle$ defined by the channel Hamiltonian H_1):

$$|\psi^{(a)}\rangle = |\Phi_{01}\rangle\delta_{a1} + G_a v_a \sum_{b\neq a} |\psi^{(b)}\rangle, \quad a = 1, 2, 3. \quad (91)$$

Now, in the wave-packet approach, we replace each Faddeev component $|\psi^{(a)}\rangle$ with its projection onto 3WP basis in the channel (a):

$$|\hat{\psi}^{(a)}\rangle = \sum_S O_S^a \big|Z_S^{(a)}\big\rangle, \quad a = 1, 2, 3, \quad (92)$$

and then one replaces exact channel resolvents $G_a = (E - H_a)^{-1}$ with their f.-d. 3WP analogs given in Eq. (84). Finally, one gets the following f.-d. equations for the Faddeev components of the "packetized" wave function:

$$|\hat{\psi}^{(a)}\rangle = \big|Z_{S_0}^{(1)}\big\rangle\delta_{a1} + \mathfrak{G}_a \mathfrak{v}_a \sum_{b\neq a} |\hat{\psi}^{(b)}\rangle, \quad a = 1, 2, 3, \quad (93)$$

where $|Z_{S_0}^{(1)}\rangle$ is the 3WP state corresponding to the initial state $|\Phi_{01}\rangle$. One of the main advantages of the momentum-lattice scheme here is that the transformation between functions in the different Jacobi sets can be expressed by a f.-d. matrix of the "permutation operator" $\mathfrak{P}^{ab} \equiv \sum_{S,S'} |Z_S^{(a)}\rangle P_{S,S'}^{ab} \langle Z_{S'}^{(b)}|$, i.e.,

$$\langle\hat{\psi}^{(b)}|\hat{\psi}^{(a)}\rangle = \sum_{S,S'} O_S^{a*} O_{S'}^b P_{S,S'}^{ab}, \quad P_{S,S'}^{ab} \equiv \big\langle Z_S^{(a)}\big|Z_{S'}^{(b)}\big\rangle, \quad (94)$$

in contrast to the direct solving of the Faddeev equations in the momentum space, where time-consuming multidimensional interpolations for scattering solution taken in different Jacobi coordinates are required in each step of the iteration. Using the expansion of the scattering packets $|Z_S^{(a)}\rangle$ on the free-packet basis similar to Eq. (89), one can express the above permutation matrix $\mathbf{P}^{ab}$ in terms of the overlap matrix for free three-body packets in different Jacobi coordinates $P_{kj,k'j'}^{0ab} \equiv \langle x_k, x_j, (a)|x_{k'}, x_{j'}, (b)\rangle$ which do not depend on the interaction and can be calculated easily (each matrix element can be found through a one-dimensional numerical integration [33]).

Thus, the wave-packet approach can provide direct solutions for the general Faddeev equations for any two-body interactions at the real energy and without any deformation of the integration path. In recent work [18], we successfully applied the WPCD approach with three-body wave packets expressed via Gaussian basis for solving the Faddeev equation below the breakup threshold. Very recently, we performed calculations of the nd elastic scattering up to 30 MeV with local Malfliet-Tjon NN potentials [33] which used the free momentum lattice basis for the representation of the three-body wave packets and obtained very good agreement (both below and above the breakup threshold) with the benchmark results found with the traditional Faddeev calculations. So, the WP technique with momentum lattice representation looks quite universal and convenient for practical applications to general three-body scattering problems.

VII. SUMMARY

In the present work, we have developed the general continuum discretization technique based on the analytical lattice representation for the basic scattering operators. The new technique continues investigations of L_2-type methods in atomic [5–10] and nuclear [11,21–24] physics and employs effectively stationary wave packets as a very convenient L_2 basis for the reformulation of scattering problems in terms of the discretized matrix analogs of the scattering integral equations (of the three-body Lippmann-Schwinger and Faddeev type). The main advantages of the wave-packet technique are following:

(i) Instead of the direct solution of the scattering equations in the coordinate or momentum space, we use purely matrix equations which include a matrix representation in the lattice basis for all the scattering operators. So, the method allows us to use any complicated interaction potentials, i.e., nonlocal or tensor ones, with the same general framework as simple local interactions.

(ii) As the method uses the f.-d. approximations for three-body channel resolvents with a proper behavior in complex energy plane, the WP technique is applicable in the same way both below and above three- or few-body breakup thresholds.

[14] We omit in this subsection partial wave indices.

(iii) The reduction from the initial integral scattering equations to their matrix analogs in the lattice basis can be considered as some effective regularization of these equations owing to averaging their kernel singularities over lattice cells. Therefore the solution can be constructed directly at the real energy without any deformation of the integration path into the complex momentum plane.

(iv) The wave-packet solutions have been shown to converge to the respective exact solutions of the integral equations with compact and noncompact kernels.

(v) The long-range Coulomb interaction can be included by introducing the special Coulomb wave-packet basis. The general calculation scheme remains to be the same as for the short-range interaction [17].

(vi) Due to the use of the integral version of the scattering theory, one can directly generalize the lattice technique to the solution for the few-body scattering problems (when the number of particles is more than three), the analytical finite-dimensional representation for the channel resolvents in the lattice bases being easily derived.

Thus, to summarize all these arguments, one can conclude that the WP technique can be applied favorably to numerous problems in nuclear, atomic, and molecular physics where it greatly facilitates many precise calculations. Also, this technique can be applied advantageously to other branches of the quantum physics, e.g., to the direct numerical solving of the relativistic two- and three-body Bethe-Salpeter equations with appropriate smoothing of the complex singularities in their kernels.

ACKNOWLEDGMENTS

The authors greatly appreciate partial financial support from the DFG (Grant No. 436 RUS 113/790/0-2) and RFBR (Grant Nos. 07-02-00609 and 08-02-91959), and support from the Russian Presidential grant for young scientists MK-202.2008.2.

[1] A. Deltuva and A. C. Fonseca, Phys. Rev. C **76**, 021001(R) (2007).
[2] R. Lazauskas and J. Carbonell, Phys. Rev. C **70**, 044002 (2004).
[3] H. Witala, W. Glockle, J. Golak, A. Nogga, H. Kamada, R. Skibinski, and J. Kuros-Zolnierczuk, Phys. Rev. C **63**, 024007 (2001).
[4] V. M. Suslov and B. Vlahovic, Phys. Rev. C **69**, 044003 (2004).
[5] E. J. Heller, Phys. Rev. A **12**, 1222 (1975).
[6] J. R. Winick and W. P. Reinhardt, Phys. Rev. A **18**, 910 (1978); **18**, 925 (1978).
[7] H. A. Yamani and M. S. Abdelmonem, J. Phys. B **30**, 1633 (1997).
[8] I. Bray, D. A. Konovalov, and I. E. McCarthy, Phys. Rev. A **43**, 1301 (1991).
[9] I. Cacelli, R. Moccia, and A. Rizzo, Phys. Rev. A **57**, 1895 (1998) and references therein.
[10] Z. Papp, C-.Y. Hu, Z. T. Hlousek, B. Kónya, and S. L. Yakovlev, Phys. Rev. A **63**, 062721 (2001); P. Doleschall and Z. Papp, Phys. Rev. C **72**, 044003 (2005).
[11] J. M. Bang, A. I. Mazur, A. M. Shirokov, Yu. F. Smirnov, and S. A. Zaytsev, Ann. Phys. (NY) **280**, 299 (2000).
[12] S. Quaglioni, W. Leidemann, G. Orlandini, N. Barnea, and V. D. Efros, Phys. Rev. C **69**, 044002 (2004).
[13] E. P. Wigner, *Group Theory and Its Application to the Quantum Mechanics of Atomic Spectra* (Academic, New York, 1959).
[14] A. Messiah, *Quantum Mechanics* (North-Holland, Amsterdam, 1965).
[15] O. A. Rubtsova, V. I. Kukulin, and A. M. Moro, Phys. Rev. C **78**, 034603 (2008).
[16] V. I. Kukulin and O. A. Rubtsova, Theor. Math. Phys. **130**, 54 (2002); **134**, 404 (2003).
[17] V. I. Kukulin and O. A. Rubtsova, Theor. Math. Phys. **145**, 1711 (2005).
[18] V. I. Kukulin, V. N. Pomerantsev, and O. A. Rubtsova, Theor. Math. Phys. **150**, 403 (2007).
[19] O. A. Rubtsova and V. I. Kukulin, Phys. At. Nucl. **70**, 2025 (2007).
[20] V. I. Kukulin and O. A. Rubtsova, Phys. Rev. C **76**, 047601 (2007).
[21] N. Austern, C. M. Vincent, and J. P. Farrell, Ann. Phys. (NY) **96**, 333 (1976); **114**, 93 (1978).
[22] R. Kozack and F. S. Levin, Phys. Rev. C **36**, 883 (1987).
[23] T. Matsumoto, T. Kamizato, K. Ogata, Y. Iseri, E. Hiyama, M. Kamimura, and M. Yahiro, Phys. Rev. C **68**, 064607 (2003).
[24] I. J. Thompson, in *Scattering*, edited by E. R. Pike and P. C. Sabatier (Academic, New York, 2001), p. 1360.
[25] I. H. Sloan and W. E. Smith, Numer. Math. **30**, 415 (1978).
[26] C. T. Corcoran and P. W. Langhoff, J. Math. Phys. **18**, 651 (1977).
[27] R. G. Newton, *Scattering Theory of Waves and Particles* (McGraw-Hill, New York, 1966).
[28] F. Perey and B. Buck, Nucl. Phys. **32**, 353 (1962).
[29] E. W. Schmid and H. Zeigelmann, *The Quantum Mechanical Three-Body Problem* (Vieweg, Braunschweig, 1974).
[30] H. Kamada, Y. Koike, and W. Gloekle, arXiv:nucl-th/0301018.
[31] I. H. Sloan, Nucl. Phys. **A168**, 211 (1971).
[32] N. M. Larson and J. H. Hetherington, Phys. Rev. C **9**, 699 (1974).
[33] V. N. Pomerantsev, V. I. Kukulin, and O. A. Rubtsova, Phys. Rev. C **79**, 034001 (2009).